

Plasma Lenses: Possible alternative OMD at the ILC¹

Manuel Formela^a, Niclas Hamann^a, Klaus Flöttmann^b, Gudrid Moortgat-Pick^{a,b}, Sabine Riemann^c, Andriy Ushakov^a

^a University of Hamburg, Luruper Chaussee 149, D-22761 Hamburg, Germany

^b Deutsches Elektronen-Synchrotron (DESY), Notkestrae 85, D-22607 Hamburg, Germany

^c Deutsches Elektronen-Synchrotron (DESY), Platanenallee 6, D-15738 Zeuthen, Germany

Abstract

In the baseline design of the International Linear Collider (ILC) an undulator-based source is foreseen for the positron source in order to match the physics requirements. The recently chosen first energy stage with $\sqrt{s} = 250$ GeV requires high luminosity and imposes an effort for all positron source designs at high-energy colliders. In this paper we perform a simulation study and adopt the new technology of plasma lenses to capture the positrons generated by the undulator photons and to create the required high luminosity positron beam.

arXiv:2003.03138v2 [physics.acc-ph] 10 Mar 2020

¹Talk presented at the International Workshop on Future Linear Colliders (LCWS2019), Sendai, Japan, 28 October-1 November 2019.

1 Motivation

The International Linear Collider (ILC) as well as the multi-Tev high-energy collider design CLIC have to provide polarized beams at high intensity as well as at high energy. Challenging is the production of the high-intense positron beams. The ILC uses an undulator-based positron source in the baseline design [1, 2, 3] that even produces a polarized positron beam. In this way, i.e. offering both high intense and highly polarized electron and positron beams, the physics potential of the ILC is optimized and well prepared for high precision physics as well as for any new discoveries [4, 5]. Currently an initial energy of $\sqrt{s} = 250$ GeV is discussed [6], where the undulator scheme can be applied as well [7, 8]. It has been shown that the physics precision requirements can not be fulfilled if only polarized electrons were available since in that case the systematic uncertainties get too large, see [9, 10, 11].

Since the luminosity requirements are challenging for any kind of positron sources at a high-energy colliders we study in the following a new idea, namely using a plasma lens (PL) as optic matching device instead of the commonly used quarter-wave transformer (QWT). The use of a plasma lens as an optical matching device (OMD) at the positron source is a novel application with a high potential to improve the yield and the quality of the positron bunch. We work out first design parameters of such a PL and compare the results with those from a QWT [1, 2, 12, 13].

2 Current Design: Quarter-wave transformer

2.1 Status QWT at ILC with $\sqrt{s} = 250$ GeV

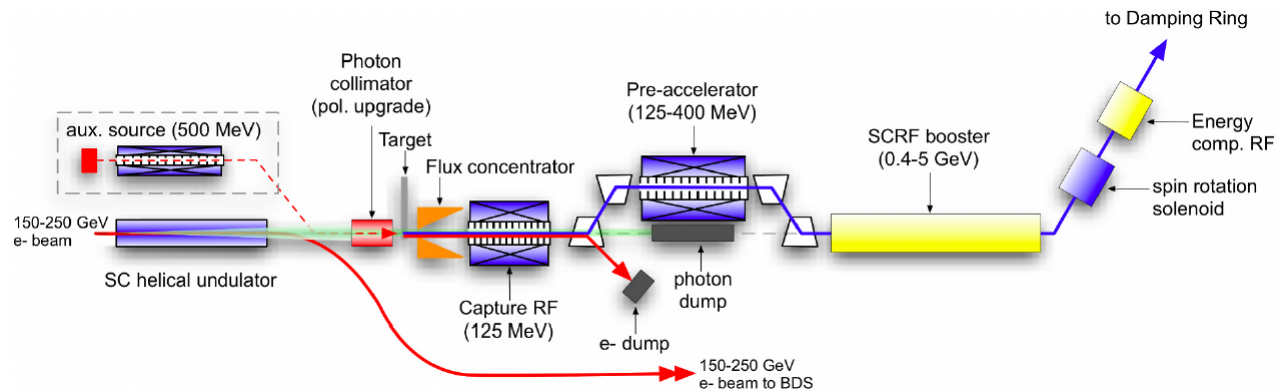


Figure 1: Schematic layout of positron source [1]

In this section we simulate the current scheme, using a quarter-wave transformer as OMD, with our tools and compare the results with results from [12, 13].

Figure 1 shows the schematic layout of the ILC positron source including the production, capture and transfer of the positron beam: electron bunches accelerated to energies between 125 – 250 GeV are injected into the helical undulator. The helical undulator is a periodic arrangement of electromagnets designed to force the electrons onto a helical trajectory, irradiating circularly polarized photons into a cone in forward direction due to the transverse accelerating process. While the electron bunch is redirected to the beam delivery system (BDS), the radiated photons are led through a photon-collimator —increasing the mean polarization— onto a rotating Ti-6%Al-4%V target. Inside the target electroweak interactions between atoms and photons

with energies above a lower limit result in pair production of longitudinally polarized electrons and positrons. Only the positrons are kept; the parameters of these still divergent positrons are required to be matched to the acceptance requirements of the downstream damping ring. This matching can be achieved with the optical matching device (OMD), which in this case is currently foreseen to be either a quarter-wave transformer (QWT) or a flux concentrator (FC). The OMD is followed by the capture RF cavity, which accelerates the positron bunch to 125 MeV. Further downstream elements before the damping ring are the electron and photon dump, SCRF booster, spin rotation solenoid, energy compression structure, cf. Figure 1 [14, 1].

2.2 Comparison of the results for the QWT

The QWT is a solenoid encased in a tapered iron shell used to capture the divergent positron shower leaving the target and presents the heart of the OMD. The shell is needed to minimize eddy currents induced in the rotating target by the magnetic field of the OMD.

Before simulating the various plasma lenses designs as OMD and examine their effectiveness, efficiency, limits, etc. as an OMD for the ILC, we use the program ASTRA [15] for simulating the QWT device. We benchmarked our simulations on a QWT design, discussed and simulated in GEANT4 [12, 13], for the following three reasons:

- verification of the current QWT simulations [12, 13];
- understanding of existing analyses of various positron beam properties;
- obtaining reference results for plasma lens originating from the same simulation program (ASTRA).

In the following, the QWT geometry [12] and its magnetic field used for the QWT-simulation results below are described. The QWT is located 7.6 mm from the rear side of the target and 40 mm from the front side of the RF cavity solenoid [13]. Its iron casing's front side opening is 1.1 cm in radius and is linearly tapered to 11.6 cm over a distance of 2 cm, followed by two sections of constant radii of 22 cm over 7.9 cm and 11.6 cm over 2.1 cm, respectively, where the solenoid itself sits within the former (see figure 2)[12].

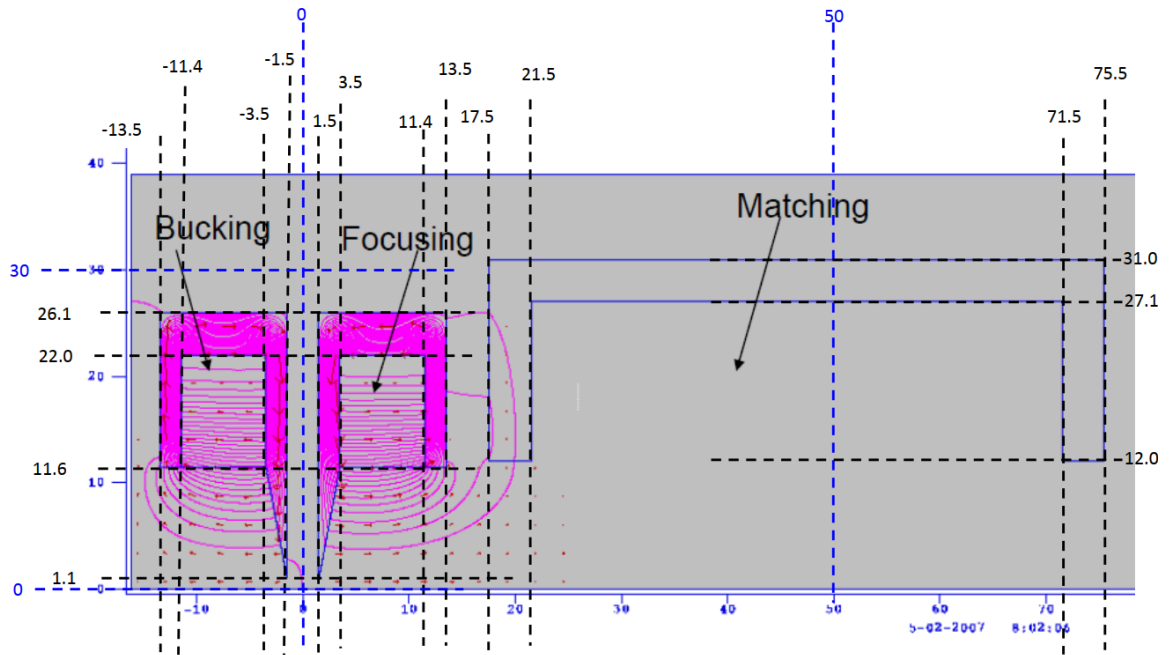


Figure 2: Geometry of the simulated QWT (focusing solenoid) nestling between the bucking and matching solenoid (lengths in cm) [12].

The on-axis longitudinal magnetic field $B_z(r = 0)$ of the QWT —,while also taking the solenoid along the RF cavities into account,— can be approximated by sections of constant, linearly increasing and linearly decreasing magnetic fields (see figure 3). The field starts with 0T at the target’s rear side, then increases linearly to 1.04T at the front side of the QWT. A constant field of 1.04T is assumed to approximate the field across the whole QWT length, followed by a section of linear decrease to 0.5T at the front side of the RF cavity. The final bit of the magnetic field, located across the RF cavity, is constant and achieves 0.5T [13]. Declaring only the on-axis longitudinal magnetic field values is sufficient to run the simulations, because the radial dependency as well as the radial magnetic field component can be derived from a polynomial expansion [16].

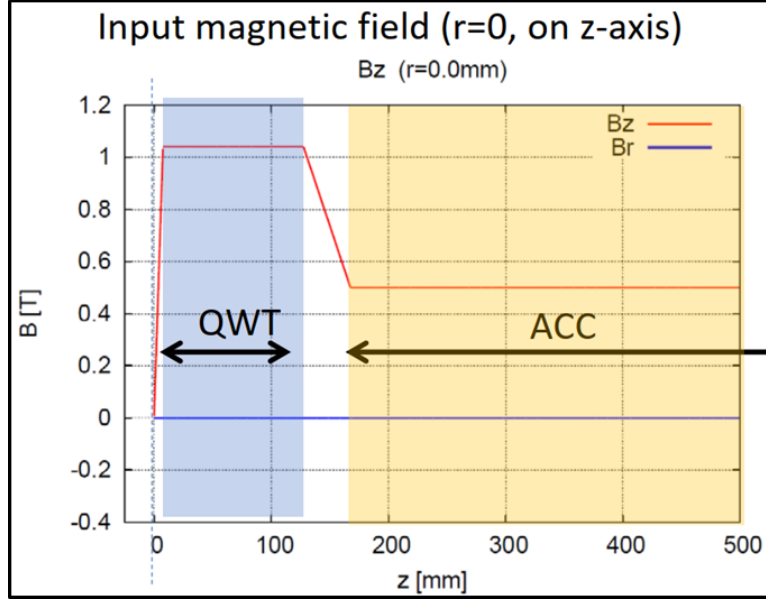


Figure 3: The approximated on-axis longitudinal magnetic field of the QWT including the solenoid from the cavity section [13].

The QWT simulation, presented now, does not consider space charge effects, i.e. the Coulomb interaction within the positron bunch. It has been assumed, however, that the positrons are only affected by the QWT'S magnetic field and by its geometry. The used positron distribution, has been derived from GEANT4 simulations based on undulator radiation simulation in CAIN[17, 13]. The obtained results are: from the initial 42917 positrons exiting the target 33732 pass the QWT in our simulation and 35865 in those of [17], respectively. This is a difference of less than 6%. Almost all lost positrons enter the front side of the QWT.

Comparing now the positron distributions in terms of their transversal momentum p_t , divergence $\sin \theta = p_t/p_z$ and energy E reveals good agreement between both simulation approaches. The observables were always taken for every single positron at the entrance of the RF cavity solenoid, exactly 40mm away from the QWT'S rear side, cf. the case that the positron beam was dumped onto a target exactly at this position.

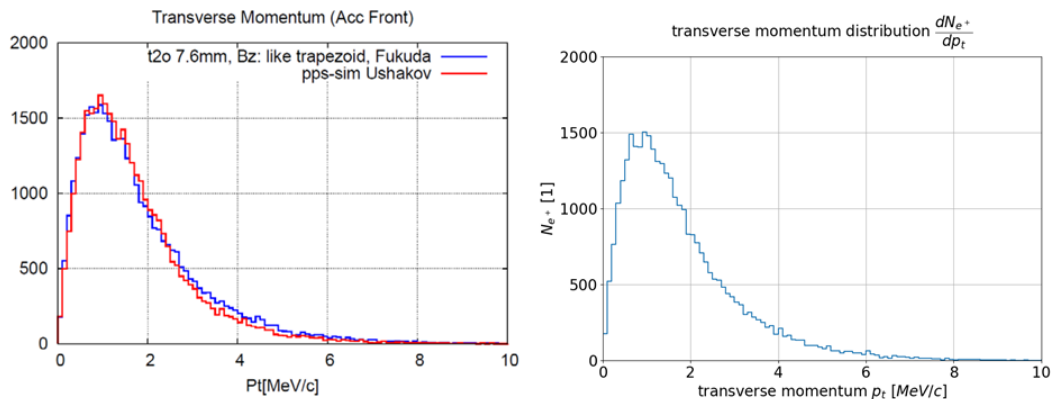


Figure 4: Comparison of the transversal momentum distribution of the positron bunch at the entrance of the cavity solenoid (right panel) with the corresponding results from [13] (left panel).

In figure 4 the simulated momentum distribution dN_{e^+}/dp_t with a bin size of 0.1 MeV/c is plotted (right panel) and compared with the corresponding result from [13] (left panel). Both

graphs have very similar trends, deviating only on the peak size, which can be explained by the previously stated 6% difference in the total number of positrons.

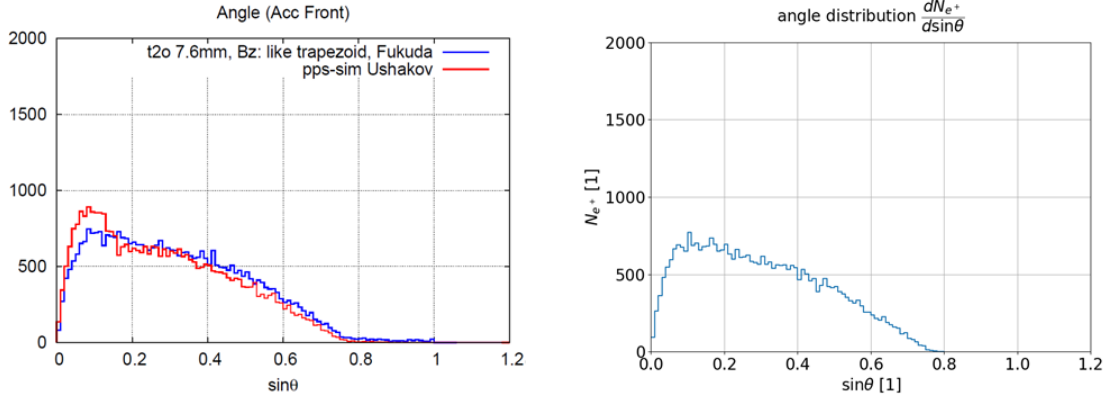


Figure 5: Comparison of the divergence distribution of the positron bunch at the entrance of the cavity solenoid (right panel) with the corresponding results from [13] (left panel).

In figure 5 the derived divergence distribution $dN_{e^+}/d \sin \theta$ with a bin size of 0.01 is plotted (right panel) and compared with the corresponding result from [13] (left panel). Again the two graphs are very similar.

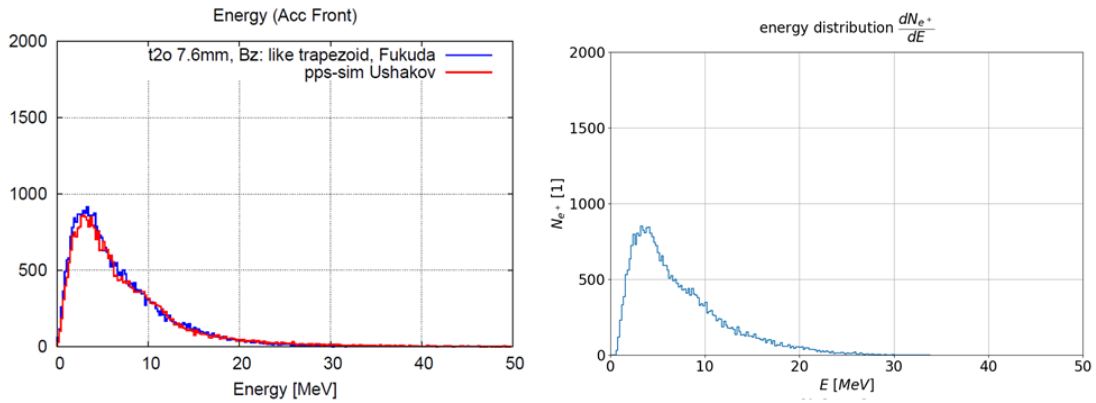


Figure 6: Comparison of the energy distribution of the positron bunch at the entrance of the cavity solenoid (right panel) with the corresponding results from [13] (left panel).

Finally, the energy distribution dN_{e^+}/dE with a bin size of 0.2 MeV is plotted in figure 5 (right panel) and compared with the corresponding result from [13] (left panel). Concerning this energy distribution both graphs are nearly indistinguishable.

Concluding our QWT simulation section, one can state that the code ASTRA has been successfully applied to simulate the OMD, cf. [13]. In the following, we therefore also use ASTRA as reference simulation for the plasma lenses.

3 Novel idea: active plasma lenses

3.1 Fundamental principles

The active plasma lens (PL) set-up consists of a capillary, filled with gas (e.g. H_2), having an electrode each attached to both opposing openings, see figure 7 (left panel) [18]. A pulser system supplies both cathode and anode with a short multi-kV voltage pulse. The strong electric

field along the capillary leads to the ionization of the gas, i.e. freeing electrons from bondings with atoms/molecules and therefore forming a gas mixture of free electrons and positively charged ions, called a plasma. Furthermore the electric field also accelerates the free electrons in the direction of the cathode leading to a strong sub- μs axial discharged current pulse in the order of up to some hundreds of Ampere, see figure 7 (right panel). The moving charge induces an azimuthal magnetic field —similar to a wire— which then in turn allows for a radially symmetric focussing of charged particle beams passing the capillary and accordingly also the plasma with negligible interaction.

One should note that any kind of windows, that would be vulnerable to drastic stress from the positron beam, are obsolete in the case at hand due to the use of differential pumping of the capillary gas.

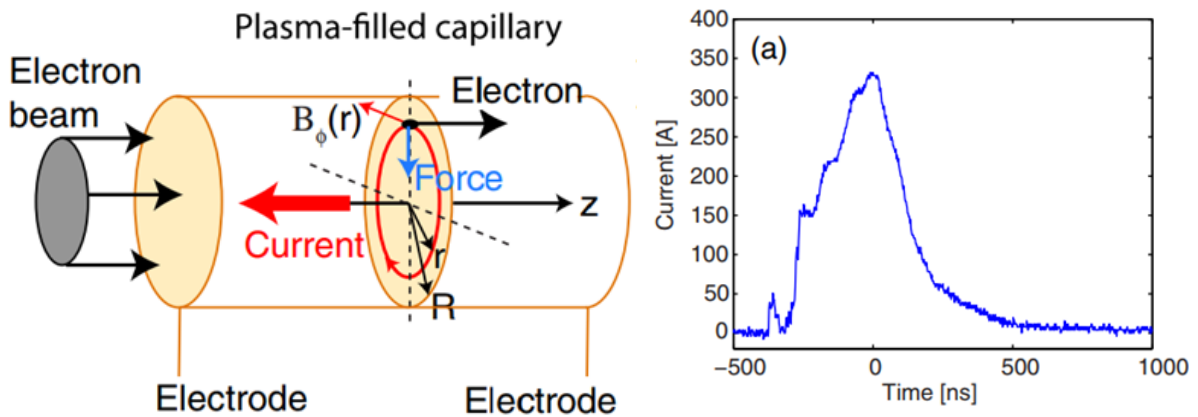


Figure 7: The principle of an active plasma lens (left panel) and the characteristic discharge current pulse in plasma lenses (right panel) [18].

3.2 Design results

In order to get a parallel beam from such a rather divergent positron beam, mentioned above, one has to use an decreasing magnetic field along the z -axis, applying, for instance, such tapered plasma lenses. These lenses vary their radius along the z -axis, which results in altering the magnetic field. These lenses belong to the class of adiabatic matching device (AMD) for focusing electron/positron beams. It is the specific manner how the magnetic field decreases that made tapering of plasma lenses appear to be the right approach to apply PLs as an OMD[19]. The basic elements of future designs will consist of a tapered and a constant plasma lens. This combination of tapered plasma lens followed by a constant plasma lens will be referred as device.

With regard to the OMD for the positron source of the ILC we finally came up —after varying many parameters— with a first design proposal. It consists of a down tapered plasma lens and a constant lens, which was previously demonstrated experimentally to work in principle as one integrated device[19]. Both lenses are 3 cm long and the constant one immediately starts after the tapered plasma lens. The tapered plasma lens starts at $z = 7.6\text{mm}$ with a radius of 10 mm which expands linearly to 25 mm within 30 mm. The constant one has the radius 25 mm. All in all the whole device is only 60 mm long and the current strength is set to 2500 A, cf. Table 1, more details see [20].

Total number of particles on stack	1000
Positrons	1000
particles at the cathode	0
active particles	766
passive particles (lost out of bunch)	0
probe particles	0
backward traveling particles	28
particles lost with $z < Z_{\min}$	0
particles lost due to cathode field	0
particles lost on aperture	234

Table 1: Plasma lens as design for the OMD for the ILC positron source (more details, see [20]).

In our simulation with the ASTRA code, the space charge is neglected in first approximation and only the interaction between particle and magnetic field has been taken into account, similar as in the previous case when benchmarking the code with the simulation for the QWT.

The following beam statistics are calculated up to 15 mm after the device ended, i. e. at the final position $z = 9.26$ cm. As can be seen in table 1 766 positrons from the initial 1000 simulated positrons are still active at this point, meaning they were not lost on the plasma lens geometry. It is important to note, however, that some of the active particles also travel backwards. This decreases the effective active particle count slightly to 738 positrons when measuring the statistics.

Particles taken into account N	766
total charge Q	1.22E-07 nC
horizontal beam position x	0.15 mm
vertical beam position y	0.31 mm
longitudinal beam position z	9.26E-02 m
horizontal beam size sig x	15.71 mm
vertical beam size sig y	16.92 mm
longitudinal beam size sig z	25.68 mm
average kinetic energy E	6.78 MeV
energy spread dE	5259 keV
average momentum P	7.27 MeV/c
transverse beam emittance eps x	2.11E+04 pi mrad mm
transverse beam emittance eps y	2.11E+04 pi mrad mm
longitudinal beam emittance eps z	1.31E+05 pi mrad mm

Table 2: Plasma lens design (more details, see [20]).

In table 2 one can see the general beam statistics which consists of the spatial position, the beam size, the emittance in all three dimensions.

In Figures 8, we show the so-called z-plots of the discussed plasma lenses: the horizontal axis represents the z-position longitudinal to the beam and the vertical axis represents the transversal position of each particle. There black dots belong to active particles, red dots belong to particles lost on the geometry and blue dots denote particles that are set inactive via leaving the minimum z-position by travelling backwards.

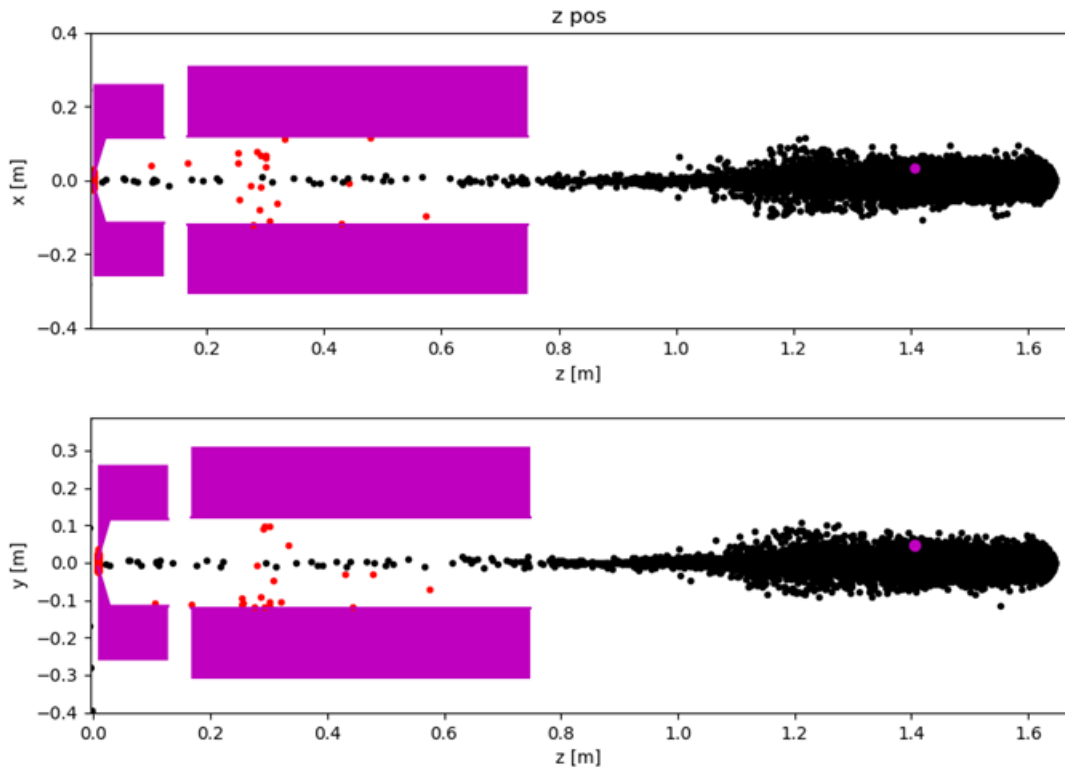


Figure 8: Zplot of a plasma lens. Black dots belong to active particles and red dots belong to particles lost on the geometry.

In the future we will further look into different plasma lens designs including also the damping ring acceptance and experimental feasibility. Also some parts of the RF cavities that are leading up to the damping ring are to be included, turning our simulations more sophisticated and still more appropriate, cf. [20, 21]. However, already these first benchmarking simulations point to promising results for using plasma lenses as AMDs.

4 Prospects and conclusions

When compared to the quarter-wave transformer the plasma lens design in our simulation study has a similar and even better positron yield than the quarter-wave transformer, since it is the effective field component which focuses the beam. Because of this the design of a plasma lens would be much smaller than a quarter-wave transformer. The total length of the quarter-wave transformer is 12 cm [13], whereas the plasma lens only needs 6 cm. This study is still ongoing, however the results are very promising and should be pursued. The next steps are to include the damping ring acceptance and to address also some technical aspects. One should note that plasma lenses are an active field right now and many experiments are ongoing, as FLASHForward at DESY that will investigate, for instance, the stability of plasma for long pulse operation which is also of relevance for our study. Therefore it can not yet be stated that the plasma lens is actually superior as OMD. Furthermore, one should keep in mind that in addition to capture efficiency, also technical feasibility, reliability and costs are important

factors as well. It is expected that not only the field of positron sources for high-energy colliders will benefit from new developments in plasma lenses.

Acknowledgements

GMP acknowledges by the Deutsche Forschungsgemeinschaft (DFG German Research Foundation) under Germany's Excellence Strategy –EXC 2121 "Quantum Universe" – 390833306.

References

- [1] C. Adolphsen *et al.*, arXiv:1306.6328 [physics.acc-ph].
- [2] ILC Reference Design Report, <http://www.linearcollider.org/ILC/Publications/Reference-Design-Report>.
- [3] Baseline Conceptual Design of the International Linear Collider, http://www.linearcollider.org/wiki/doku.php?id=bcd:bcd_home.
- [4] G. Moortgat-Pick *et al.*, Eur. Phys. J. C **75** (2015) no.8, 371 doi:10.1140/epjc/s10052-015-3511-9 [arXiv:1504.01726 [hep-ph]].
- [5] J. A. Aguilar-Saavedra *et al.* [ECFA/DESY LC Physics Working Group], hep-ph/0106315.
- [6] K. Fujii *et al.*, "The role of positron polarization for the initial 250 GeV stage of the International Linear Collider," arXiv:1801.02840 [hep-ph].
- [7] A. Ushakov, G. Moortgat-Pick and S. Riemann, arXiv:1801.08465 [physics.acc-ph].
- [8] S. Riemann, P. Sievers, G. Moortgat-Pick, A. Ushakov, *Status of the undulator-based ILC positron source*, these proceedings.
- [9] R. Karl, PhD Thesis 'From the Machine-Detector Interface to Electroweak Precision Measurements at the ILC', University of Hamburg, February 2019.
- [10] R. Karl and J. List, arXiv:1703.00214 [hep-ex].
- [11] H. Aihara *et al.* [ILC Collaboration], arXiv:1901.09829 [hep-ex].
- [12] M. Fukuda, KEKB/SuperKEKB positron source a review and the status, AWLC2017
- [13] M. Fukuda, Undulator Positron Source Capture Simulation, LCWS2019 and private communication.
- [14] R. Pausch, Magnetic fields of the optical matching devices used in the positron source of the ILC.
- [15] K. Floettmann, ASTRA: A space charge tracking algorithm. (2011).
- [16] K. Floettmann, ASTRA user manual. (2000).
- [17] M. Fukuda, K. Yokoya, private communication.
- [18] J. van Tilborg *et al.*, Phys. Rev. Lett. **115**, 184802 (2015).

- [19] Filippi, F., et al. "Tapering of plasma density ramp profiles for adiabatic lens experiments." Nuclear Instruments and Methods in Physics Research Section A: Accelerators, Spectrometers, Detectors and Associated Equipment 909 (2018): 339-342.
- [20] N. Hamann, Bachelor Thesis, University of Hamburg, 2020, *in preparation*.
- [21] M. Formela, Master Thesis, University of Hamburg, 2020, *in preparation*.